

# Increasing Heterogeneity in the Organization of Synaptic Inputs of Mature Olfactory Bulb Neurons Generated in Newborn Rats

Wolfgang Kelsch,<sup>1</sup> Shuyin Sim,<sup>2</sup> and Carlos Lois<sup>3\*</sup>

<sup>1</sup>Department of Clinical Neurobiology, University Heidelberg, D-69120 Heidelberg, Germany

<sup>2</sup>Department of Biology, Massachusetts Institute of Technology, Cambridge, Massachusetts 02139, USA

<sup>3</sup>Department of Neurobiology, University of Massachusetts Medical School, Worcester, Massachusetts 01655, USA

## ABSTRACT

New neurons are added into the mammalian olfactory bulb throughout life, but it remains unknown whether the properties of new neurons generated in newborn animals differ from those added during adulthood. We compared the densities of glutamatergic synapses of granule cells (GCs) generated in newborn and adult rats over extended periods of time. We observed that, whereas adult-born GCs maintained stable cell-to-cell variability of synaptic densities soon after they integrated into the circuit, cell-to-cell variability of synaptic densities of neonatal-born GCs increased months after

their integration. We also investigated whether the synaptic reorganization induced by sensory deprivation occurred differently in mature neonatal- and adult-born GCs. Sensory deprivation after new GCs had differentiated induced more pronounced changes in the synaptic densities of neonatal-born GCs than in adult-born GCs. These observations suggest that the synapses of mature neonatal-born GCs retain a higher degree of malleability in response to changes in neuronal activity than adult-born GCs. *J. Comp. Neurol.* 520:1327–1338, 2012.

© 2011 Wiley Periodicals, Inc.

**INDEXING TERMS:** neurons; mammalian olfactory bulb; granule cells

It is generally believed that adult neurogenesis provides a continuous influx of immature neurons that are highly plastic only while they are integrating into brain circuits, and subsequently lose most of this plasticity necessary for storage of novel information. Adult neurogenesis could thus represent a continual addition of immature neurons with essentially the same set of properties as neurons generated in the developing brain. An alternative hypothesis is that the properties of adult-born neurons differ from those generated during neonatal development and may serve different functions in the olfactory bulb circuit.

The vast majority of new neurons added to the olfactory bulb (OB) throughout postnatal life are granule cells (GCs) that are generated in the subventricular zone (SVZ) and migrate to the GC layer where they differentiate and form synapses (Altman, 1962; Lois and Alvarez-Buylla, 1993; Luskin, 1993). GCs are axonless interneurons that receive different types of glutamatergic inputs onto synapses in distinct dendritic domains. Deprivation of sensory input during neuronal differentiation (“early deprivation”) induces changes to the synaptic densities in all

dendritic domains of adult-born GCs (Kelsch et al., 2009). In contrast, deprivation starting after these neurons have differentiated (“late deprivation”) only evokes limited synaptic reorganization. These observations suggest a critical period for activity-dependent remodeling of synapses in adult-generated GCs in line with a similar temporal window for inducibility of synaptic long-term potentiation in adult-born GCs (Nissant et al., 2009).

We previously observed that neonatal- and adult-born GCs differ in the sequence in which their synapses form while neurons mature and integrate into the circuits of the OB (Kelsch et al., 2008). However, it is not known whether mature neonatal- and adult-born GCs also differ in how they maintain their synaptic organization over

Grant sponsor: National Institutes of Health (NIH); Grant number: 5-R01-DC008870-04 (to C.L.); Grant sponsor: Deutsche Forschungsgemeinschaft (DFG); Grant number: KE1661/1-1 (to W.K.).

\*CORRESPONDENCE TO: Carlos Lois, MD, PhD, Dept. of Neurobiology, University of Massachusetts Medical School, Worcester, MA 01655. E-mail: Carlos.Lois@umassmed.edu

Received June 20, 2011; Revised September 29, 2011; Accepted October 25, 2011

DOI 10.1002/cne.22799

Published online November 18, 2011 in Wiley Online Library (wileyonlinelibrary.com)

© 2011 Wiley Periodicals, Inc.

**TABLE 1.**  
**Primary Antibodies**

Antigen	Immunogen	Source, species, mono- vs. polyclonal	Dilution used
Green fluorescent protein (GFP)	Full-length jellyfish protein	Abcam, rabbit polyclonal (AB290)	1:4,000
Bassoon	Aa 756-1,001 of rat Bassoon protein	Stressgen (Enzo Life Sciences), mouse monoclonal (clone SAP7F407)	1:750
c-Fos	Synthetic peptide corresponding to aa 4-17 of human c-Fos	Calbiochem, rabbit polyclonal (AB5)	1:10,000
Tyrosine hydroxylase	Denatured tyrosine hydroxylase from rat pheochromocytoma	Chemicon, rabbit polyclonal (AB152)	1:1,000

extended periods of time postmaturation. Here we analyze the organization of synaptic inputs to neonatal-born GCs throughout the animal's life and in response to sensory deprivation after the new neurons completed their maturation and observed that mature neonatal-born GCs retain a high degree of malleability in response to changes in neuronal activity.

## MATERIALS AND METHODS

Experiments were performed with Sprague-Dawley rats of either sex (Charles River, Portage, MI). Neonatal animals were postnatal day 5 and adult animals >56 days old at the time of injection. All animal procedures were approved by the local Animal Welfare Committee Institutional Animal Care and Use Committee (IACUC, MIT, Cambridge, MA) and in accordance with National Institutes of Health (NIH) guidelines. Animals were kept on a 12-hour daylight cycle. Experiments for neonatal- and adult-born GCs were performed in parallel and under similar conditions (same housing room, same type of ventilation cage, and two animals per cage after weaning).

### Generation of retroviral vectors

To visualize dendritic morphology we used an oncoretroviral vector derived from Moloney Leukemia virus with an internal promoter derived from the LTR from the Rous Sarcoma Virus (RSV) driving palmitoylated green fluorescent protein (GFP, called MPalmG). To visualize glutamatergic postsynaptic clusters or presynaptic release sites, we generated a vector called Mpsdg or Msygg by replacing the palmitoylated GFP from MPalmG with the ORF of PSD95:GFP or Synaptophysin:GFP, respectively. Recombinant retroviral vectors were prepared and stored as previously described (Kelsch et al., 2008).

### Stereotactic retroviral labeling

Adult animals were anesthetized by an intraperitoneal (i.p.) injection of ketamine/xylazine and neonatal animals by hypothermia. A retroviral stock solution (200 nl) was injected bilaterally in the SVZ at stereotaxic coordinates: (anterior; lateral; ventral; mm in reference to bregma with

bregma and lambda being horizontally aligned) +1.2;  $\pm 1.6$ ;  $-3.1$  for adult rats (>P56) and +0.9;  $\pm 2.1$ ;  $-2.1$  for neonatal rats (postnatal day, P5).

### Animal perfusion, histological processing, and immunohistochemistry

Rats were given an overdose of ketamine/xylazine and perfused transcardially with phosphate-buffered saline (PBS) (pH 7.2) at 37°C for 30 seconds followed by 3 minutes of 3% paraformaldehyde (PFA) and postfixed in 3% PFA for 12 hours at 4°C. 50- $\mu$ m-thick coronal slices were cut with a Leica vibratome. For genetic synaptic markers, sections were incubated in primary rabbit anti-GFP or mouse anti-Bassoon antibodies at 4°C overnight, and Alexa-555 secondary antibodies (1:750, Molecular Probes, Eugene, OR) diluted in blocking solution for 2 hours at room temperature. Blocking solution contained 0.25% TritonX and 1% bovine serum albumin. Sections were mounted with Gelmount (Sigma, St. Louis, MO).

For morphological reconstruction of the basal dendrites (Fig. 4), 100- $\mu$ m-thick coronal sections were incubated in primary rabbit anti-GFP antibody at 4°C for 2 days and Alexa-488 secondary antibody (1:750, Molecular Probes) diluted in blocking solution at 4°C overnight.

### Antibody characterization

We used the following primary antibodies (Table 1): Anti-GFP rabbit polyclonal antibody labeling was only detected in cells that also formed synaptic clusters.

Anti-Bassoon antibody has been shown to detect a band of  $\approx 400$  kDa synaptosomal fraction of rat brain by western blot (manufacturer's specification), and staining is absent in Bassoon knockout retinae (Brandstatter et al., 1999) and colocalizes to proteins in the active zone (Regus-Leidig et al., 2009).

Anti-c-Fos antibody recognizes both c-Fos and v-Fos, but does not react with the 39-kDa Jun protein (manufacturer's specification). Specificity of this same antibody has been determined by others via colocalization of the immunoprotein with c-fos mRNA and the blocking of specific staining following immunogen preabsorption (Serrats and Sawchenko, 2006).

Anti-tyrosine hydroxylase antibody has been shown to react with rat tyrosine hydroxylase, and by western blot analysis to label a single band at  $\approx 62$  kDa (reduced) corresponding to tyrosine hydroxylase (manufacturer's specification), but does not recognize other monoaminergic synthetic enzymes (Northcutt et al., 2007). Tyrosine hydroxylase labeling in the OB was restricted to the glomerular layer (data not shown) as previously described (Smeets and Gonzalez, 2000).

### Image acquisition and analysis

Confocal image stacks were acquired by using an Olympus Fluoview 300 confocal microscope (60 $\times$  oil-immersion lens [NA, 1.4]; pixel size, 0.23  $\times$  0.23  $\mu\text{m}$ ), and with z-step 0.25  $\mu\text{m}$ . A typical image stack consisted of  $\approx 80$ –150 image planes each of 1024  $\times$  1024 pixels. For each stack, laser intensity and detector sensitivity were set to the same values determined in initial experiments. After acquisition, maximal intensity projections were prepared for each image stack using Olympus acquisition software. No filtering was generally necessary. For projection images the threshold was set so that any possible diffuse GFP fluorescence at the dendritic shaft was below this threshold. The number of PSDG<sup>+</sup> clusters in a region of interest was counted by using the integrated morphometry analysis function of the MetaMorph software (Universal Imaging, West Chester, PA). The length of the respective segment of the dendritic arbor was then measured and the density of PSDG<sup>+</sup> clusters was determined. For stacks containing at least 40 single images (corresponding to a stack height of 10  $\mu\text{m}$ ), the density directly corresponded to the length of a dendrite segment measured in that stack. Increasing the number of single images (e.g., stacks of 80–150 images corresponding to a stack height of 20–37.5  $\mu\text{m}$ ) did not change the density of synaptic clusters in the same dendritic segment as compared to the stack containing only 40 single images (corresponding to a stack height of 10  $\mu\text{m}$ ).

For long-term survival, GCs were chosen based on the preservation of the dendritic tree using only the red channel (that visualized the dendritic tree, but not synaptic clusters). To account for interanimal variability, each analyzed data point (e.g., basal domain, 17 days postinfection [d.p.i.]) contained normally distributed PSDG<sup>+</sup> cluster densities from 3 GCs per animal resulting in a total of 42 cells from 14 animals per data point, except for 1-year-old adult-born GCs, of which we only found a total of 19 PSDG<sup>+</sup> cells in 8 of 11 injected animals. For adult-born neurons the number of cells surviving 1 year after injection was low, and not all the neurons were appropriate for analysis. For instance, we could not analyze neurons whose dendrites were truncated or neurons whose dendritic arbors were not oriented parallel to the histolog-

ical sections. Due to these limitations, we were only able to analyze 19 cells in the group of adult-born neurons with 1-year survival, which is lower than the number of cells (42 cells) that we used for all the other experimental groups. To test the appropriateness of investigating a group with a lower number of cells (1-year survival of adult-born neurons) we analyzed the statistics of all our timepoints using samples of 42 cells, 21 cells, or 14 cells, and observed that the mean and SD in all our groups were consistent, regardless of the number of cells used for the analysis (Table 2C). This analysis indicates that it would be appropriate to perform comparisons with a lower number of cells. Thus, for the experiments regarding the synaptic densities of neurons of adult-born neurons with 1-year survival we used the values obtained from 19 cells.

We observed more superficial adult-born GCs at 1 year than at 1 month after they had been generated (data not shown); however, due to the originally intended low labeling density for reconstructions, we did not statistically quantify for a shift toward more superficial GCs among these long-term surviving cells. As GCs with deep and superficial dendritic targeting in the external plexiform layer had comparable mean and standard deviation (SD) of synaptic densities in their dendritic domains at the respective timepoints (data not shown), data were pooled. Statistical differences in the SD were determined using a Bartlett's test and for pairwise comparisons an F-test for differences in variances (Graphpad Prism software, San Diego, CA).

For reconstruction of basal dendrite length (Fig. 4), three animals were perfused 1 month and 1 year after retroviral labeling with a retrovirus expressing palmitoylated GFP (MPalmG). Confocal stack images (z-step 2  $\mu\text{m}$ , 30 planes per stack) were acquired with an Olympus Fluoview 300 laser scanning microscope (20 $\times$  objective). Maximum density projections were generated and length of dendrites was measured using Metamorph analysis software. Data were further analyzed with IgoPro software (WaveMetrics, Lake Oswego, OR).

### Sensory deprivation

Unilateral surgical naris occlusion was performed on the day of intracerebral injection of viruses *Mpsdg* and *Msvp* into the SVZ (P5) or at the indicated timepoints. Nares were occluded by cauterization. Nares were unilaterally occluded to compare deprived and nondeprived olfactory bulbs in the same animal. As previously described for adult-born GCs (Kelsch et al., 2009), only animals that showed a strong reduction in immunofluorescences of *c-Fos* and A555-conjugated secondary antibody (1:1,000, Molecular Probes) expression in the granule cell layer and reduction of tyrosine hydroxylase and A488-conjugated

**TABLE 2.**  
Statistical Analysis of Differences in Variances (SD)

A.* Adult-born GCs: PSDG+ synapses densities		Bartlett's test	
~ Domain	Equal variances comparing all timepoints?	P-value	
Distal	yes	$P = 0.764$	
Proximal	yes	$P = 0.301$	
Basal	yes	$P = 0.318$	

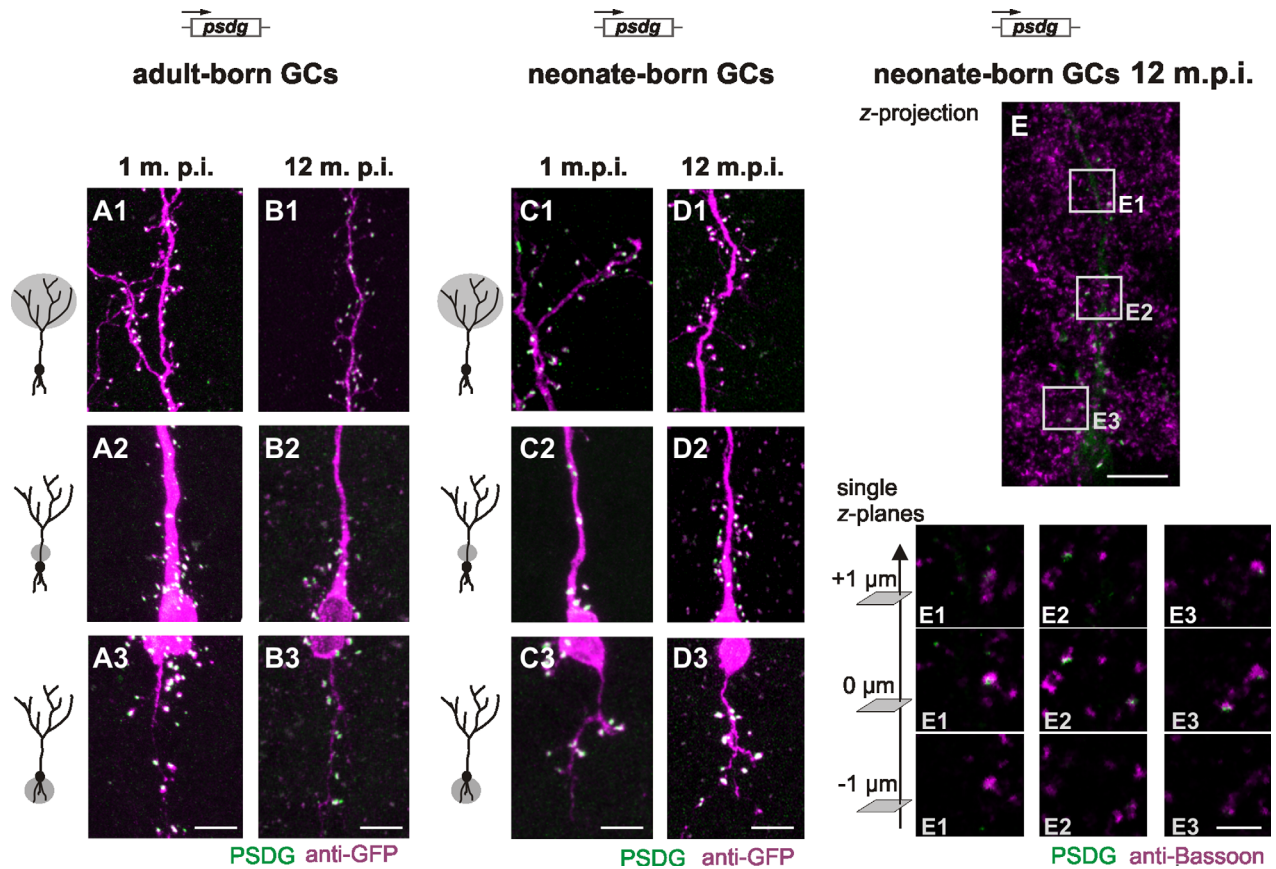
B.† Neonate-born GCs: PSDG+ synapses densities		Bartlett's test		F-test for different variances	
~ Domain	Equal variances comparing all timepoints?	P-value	1 m.p.i. vs. 2 m.p.i.	1 m.p.i. vs. 12 m.p.i.	2 m.p.i. vs. 12 m.p.i.
Distal	yes	$P = 0.764$	$P = 0.516$	$P = 0.410$	$P = 0.142$
Proximal	no	$P < 0.0001$	$P = 0.090$	$P < 0.0001$	$P < 0.0001$
Basal	no	$P < 0.0001$	$P = 0.112$	$P = 0.0024$	$P < 0.0001$

C. Neonate-born GCs: PSDG+ synapses densities: Comparison of variance at the same maturation stage		F-test for different variances					
~ Domain	Mean $\pm$ SD	Split data: 1 m.p.i.		Split data: 2 m.p.i.		Split data: 12 m.p.i.	
		A (n=21)	B (n=21)	A (n=21)	B (n=21)	A (n=21)	B (n=21)
Distal	$0.331 \pm 0.102$	$0.348 \pm 0.069$	$0.369 \pm 0.094$	$0.342 \pm 0.057$	$0.373 \pm 0.110$	$0.381 \pm 0.088$	$P = 0.513$
Proximal	$0.352 \pm 0.112$	$0.327 \pm 0.091$	$0.378 \pm 0.162$	$0.323 \pm 0.091$	$0.603 \pm 0.227$	$0.575 \pm 0.277$	$P = 0.297$
Basal	$0.299 \pm 0.101$	$0.290 \pm 0.113$	$0.302 \pm 0.092$	$0.289 \pm 0.072$	$0.369 \pm 0.176$	$0.389 \pm 0.172$	$P = 0.186$
							$P = 0.465$

\*In a total of 8 injected animals only 19 complete labeled GCs were found and analyzed.

†The pooled 12 months p.i. sample also contains the 9 months p.i. sample.



**Figure 1.** Distribution of glutamatergic input synapses in 1-year-old neonatal- and adult-born granule cells (GCs). A,B: Adult-born GCs were examined 1 (A) and 12 (B) months postinfection (m.p.i.). To attribute PSDG<sup>+</sup> clusters (green) to a particular GC, dendritic morphology was visualized by immunofluorescence with Alexa-555-labeled antibodies (shown here in magenta) against the diffuse PSDG present in the cytosol that was otherwise undetectable (Kelsch et al., 2008). The three main dendritic domains were analyzed separately (from top): distal (A1/B1), proximal (A2/B2), or basal (A3/B3) domain. C,D: Adult-born GCs were examined 1 (C) and 12 (D) m.p.i. The three main dendritic domains were analyzed separately (from top): distal (C1/D1), proximal (C2/D2), or basal (C3/D3) domain. E: Confocal maximum density projection (E) shows PSDG<sup>+</sup> clusters in a 1-year-old neonatal-born GC that are contacted by the presynaptic marker, Bassoon. The lower three image series (E1–E3) show single planes of the top projection separated in z-axis by 1  $\mu$ m. Scale bars = 10  $\mu$ m in A–E; 3  $\mu$ m in E1–E3.

secondary antibody (1:750, Molecular Probes) expression in the glomerular layer in the deprived bulb were included in further analysis (data not shown).

## RESULTS

### Protracted changes in the synaptic organization of neonatal-born GCs

We compared synaptic densities of neonatal- or adult-born GCs at 1, 2, and 12 months after they were generated in the SVZ to investigate potential long-term changes in synaptic organization (Fig. 1). Synaptic organization is defined here as the density of glutamatergic input synapses in various dendritic domains. We used oncoretroviral vectors to genetically label synapses in new GCs, because retroviral labeling allows reliable birth-dating of new neurons (Sanes, 1989). To measure the

density of glutamatergic input synapses, we delivered PSDG, a genetic marker consisting of a fusion protein between PSD-95 and GFP. To attribute PSDG<sup>+</sup> clusters (green fluorescence) to a particular GC, dendritic morphology was visualized by immunofluorescence with red labeled antibodies against the diffuse PSDG present in the cytosol that was otherwise undetectable (Kelsch et al., 2008). PSD-95 is a protein localized to the postsynaptic density of glutamatergic input synapses (Sheng, 2001). PSDG delivered into new neurons with retroviral vectors (*Mpsdg*) can be used to genetically label these synapses (Niell et al., 2004; Gray et al., 2006; Kelsch et al., 2008, 2009; Livneh et al., 2009; Sturgill et al., 2009), and expression of PSDG at modest levels produced by retroviral expression does not alter synaptic properties as measured by electrophysiological methods (Kelsch et al., 2008). PSDG<sup>+</sup> clusters were contacted by

the presynaptic protein Bassoon both in immature (Kelsch et al., 2008) and 1-year-old GCs (Fig. 1E), and PSDG was clustered at asymmetric synapses on an ultrastructural level (Livneh et al., 2009).

We examined the densities of glutamatergic synapses in different dendritic domains of GCs. The apical dendrite can be divided into an unbranched segment emerging from the soma (the proximal 15% of this unbranched segment is referred to as the proximal domain; Kelsch et al., 2008) followed by a branched segment (distal domain). The proximal domain and basal dendrite (basal domain) receive axodendritic glutamatergic input from axon collaterals of the OB's projection neurons and from axons originating in the olfactory cortices (Mori, 1987). Synapses present in the distal domain of the apical dendrite are bidirectional dendrodendritic synapses where input and output synapses are colocalized and functionally coupled. These synapses receive glutamatergic input from the lateral dendrites of the OB's projection neurons and release GABA back onto these same projection neurons (Mori, 1987).

We compared the densities of input synapses in neonatal- or adult-born GCs 1, 2, and 12 months after they had been generated in the SVZ (Fig. 1). We observed that the variability (SD) of densities of PSDG<sup>+</sup> synapses in the different dendritic domains of adult-born GCs did not change between 1, 2, and 12 months after they were generated (Fig. 2A; Table 2A). Similarly in neonatal-born GCs, the variability (SD) of densities of PSDG<sup>+</sup> synapses did not change in the distal domain over time (Fig. 2B1; Table 2B). Interestingly, the variability (SD) of densities of PSDG<sup>+</sup> synapses in neonatal-born GCs increased in the proximal and basal domain between the early timepoints (1- and 2-month-old GCs) and 1 year after their birth (Fig. 2B; Table 2B). The increase in variability (SD) of synaptic densities, however, was only significant for the 1-year timepoint as 1- and 2-month-old GCs displayed similar variability (SD).

As we compared 1- to 2-month- and 1-year-old GCs in different animals, we validated whether variability of densities of PSDG<sup>+</sup> clusters is not biased for the same maturation stage (e.g., 1-month-old neonatal-born GCs) by variability in our experimental conditions over time. We therefore labeled new GCs at P5 in separate groups of animals in parallel to the 1-year observation period of animals shown in Figure 1 and examined neonatal-born GCs 1 month after they had been generated. Their variability (SD) of PSDG<sup>+</sup> synapses did not significantly differ (SD: basal  $\approx$ 0.088 vs. 0.073, n.s.; proximal  $\approx$ 0.101 vs. 0.101, n.s.; distal domain 0.073 vs. 0.111, n.s., Bartlett's test, each  $n = 14$  GCs). In addition, splitting the datasets of Figure 2 into two groups of seven animals each did not reveal any difference in the variability (SD) of PSDG<sup>+</sup>

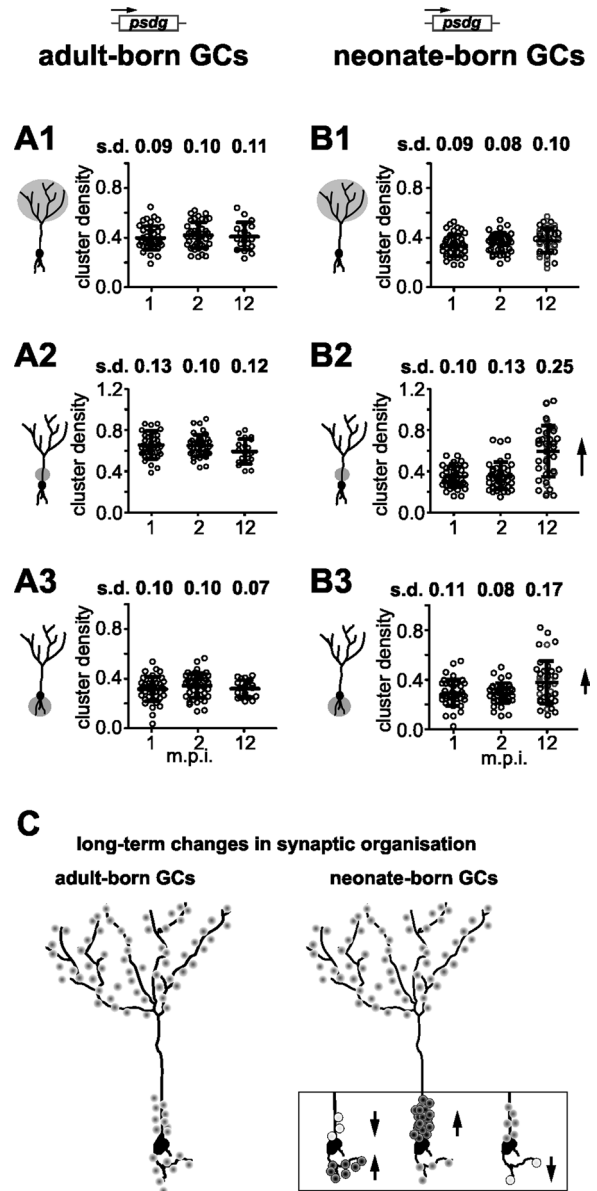


**Figure 2.** Neonatal-born GCs show an increasing variability in densities of input synapses in axodendritic input domains over time. **A:** The graphs show for each dendritic domain scatterplot of PSDG<sup>+</sup> clusters (clusters/ $\mu$ m) of adult-born GCs 1, 2, and 12 m.p.i. (42 GCs each except for 12-month-old adult-born GCs ( $n = 19$ )). The three main dendritic domains were analyzed separately (from top): distal (A1), proximal (A2) or basal (A3) domain. Mean  $\pm$  SD are plotted in red and SD values are indicated above each timepoint. Significant increases in the SD over time were determined with Bartlett's test ( $P$ -values are indicated if  $P < 0.05$ ) and are indicated by arrows (for statistical analysis see Table 2). **B:** Same as A, but for neonatal-born GCs. Twenty-eight GCs from 12 m.p.i. and 14 GCs of 9 m.p.i. were pooled for the late timepoint of neonatal-born GCs. **C:** Adult-born GCs acquire their final density of synapses within 1 month after being generated, and the cell-to-cell variability in their synaptic densities does not increase thereafter. Even months after neonatal-born GCs had been generated, they have not completely acquired a final density of synapses and the values of their synaptic densities in their basal and proximal domains become highly variable from cell to cell.

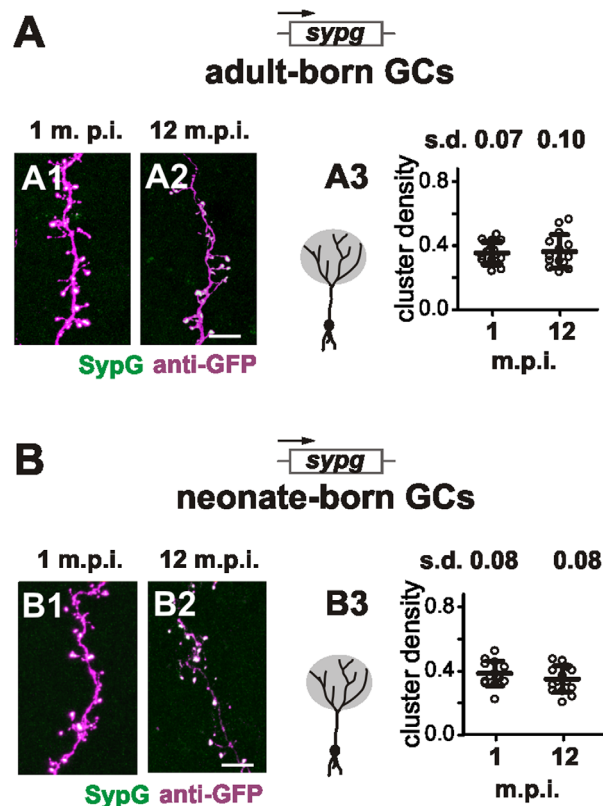


**Figure 3.** The density of output synapses does not change after maturation of adult- or neonatal-generated GCs. **A:** Synaptophysin:GFP<sup>+</sup> (SypG) clusters were examined in the distal domain of adult-born GCs 1 (A1) and 12 (A2) m.p.i. Scatterplot (A3) of densities of SypG<sup>+</sup> clusters (clusters/ $\mu\text{m}$ ) of adult-born GCs 1 and 12 m.p.i. Variances at the two timepoints did not significantly increase ( $P = 0.15$ , F-test). **B:** Synaptophysin:GFP<sup>+</sup> (SypG) clusters were examined in the distal domain of neonatal-born GCs 1 (B1) and 12 (B2) m.p.i. Scatterplot (B3) of densities of SypG<sup>+</sup> clusters (clusters/ $\mu\text{m}$ ) of neonatal-born GCs 1 and 12 m.p.i. Variances at the two timepoints did not significantly increase ( $P = 0.84$ , F-test). Scale bars = 10  $\mu\text{m}$ .

synapses for the same maturation stage (Table 2C). Finally, we tested whether neonatal-born GCs would increase cell-to-cell variability shortly after the animal reached adulthood ( $\geq P56$ ). We therefore examined the variability (SD) of densities of PSDG<sup>+</sup> synapses of neonatal-born GCs 4 months after they had been generated (mean  $\pm$  SD: basal  $\approx 0.324 \pm 0.116$ , proximal  $\approx 0.458 \pm 0.176$ , distal domain  $0.352 \pm 0.109$  PSDG<sup>+</sup> cluster/ $\mu\text{m}$ ,  $n = 14$  GCs). Variability (SD) of synaptic densities of 4-month-old GCs was not significantly different from 1- and 2-month-old GCs described in Figure 2 (Bartlett's test), further suggesting a slow increase of variability over time between 1 month and 1 year of survival.

To investigate changes in densities of output synapses over time, we labeled them using SypG, a fusion protein between Synaptophysin and GFP (Fig. 3). Syn-

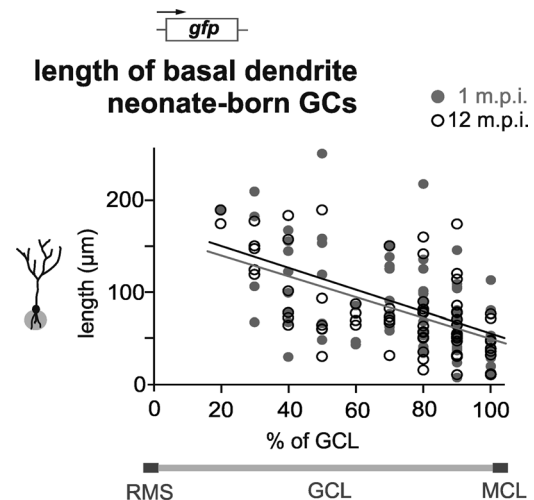


**Figure 4.** Length of basal dendrite in 1-month- and 1-year-old neonatal-born GCs. The length of the basal dendrite of neonatal-born GCs labeled 1 and 12 months after labeling with a retrovirus expressing a membrane-tagged GFP was measured (70 GCs). The length of the basal dendrite was plotted against the relative position of the soma in the GC layer. GC layer was divided in percentages, with 0% being the rostral migratory stream in the center of the bulb and 100% being the mitral cell layer.

aptophysin is a protein localized to presynaptic neurotransmitter vesicles (Sudhof and Jahn, 1991) and SypG expressed with retroviral vectors (Msypg) can be used to genetically label output synapses (Kelsch et al., 2008, 2009; Meyer and Smith, 2006). Output synapses of GCs are located in their distal dendritic domain, and they are part of dendrodendritic synapses (Hinds, 1970). We observed that variability (SD) of densities of SypG<sup>+</sup> clusters were stable between 1 month and 1 year for both neonatal- and adult-born GCs (n.s., F-test; Fig. 3), consistent with stability of PSDG<sup>+</sup> synapses in the distal domain.

We followed up on this finding by analyzing whether the increased variability in the synaptic density in the basal dendrite of neonatal-born GCs after maturation was accompanied by changes in its arbor length. We observed no significant difference in the length of the dendritic arbor length of the basal domain or its variability between samples of neonatal GCs that were either 1-month- or 1-year-old (median [interquartile range]: 77.5 [48.3–123.8]  $\mu\text{m}$  and 70.7 [50.3–105.2]  $\mu\text{m}$ ,  $n = 70$  GCs respectively, Mann-Whitney test:  $P = 0.48$ , F-test:  $P = 0.51$ , Fig. 4). We also found that the increase in variability of synaptic density in the proximal and basal domains occurred to the same degree in neonatal-generated GCs regardless of whether they had dendrites branching in the deep or superficial layers of the OB (data not shown).

In summary, the cell-to-cell variability in synaptic densities does not significantly increase in adult-born GCs after they acquire their final synaptic density within a month after being generated. In contrast, synaptic densities in the basal and proximal domains of neonatal-born GCs become increasingly variable between cells even up to 1 year after their birth.

### Sensory deprivation continues to change the synaptic organization of mature neonatal-born GCs

Neonatal- and adult-born GCs differ in the patterns in which they develop synapses in their dendritic domains during maturation (Kelsch et al., 2008), and long-term reorganization of synapses in certain dendritic domains after maturation. Do neonatal- and adult-born GCs also differ in the manner in which their synapses are affected by manipulations of sensory input? GCs are part of a sensory relay circuit, and we recently observed that immature adult-born GCs change the synaptic densities of all dendritic domains when sensory input is blocked during their differentiation (“early deprivation”) (Kelsch et al., 2009). We thus examined how the synaptic organization of immature neonatal-born GCs changes when deprived of sensory input.

We induced early sensory deprivation by performing unilateral naris occlusion at P5 when viral vectors were delivered to label new GCs in the SVZ (Fig. 5A), and subsequently examined the synaptic organization of new neonatal-born GCs using the PSDG and SypG markers (*Mpsdg* and *Msygg*, respectively). After sensory deprivation, significantly fewer PSDG<sup>+</sup> input synapses were present in the distal and basal dendritic domains (Fig. 5A). In addition, the density of SypG<sup>+</sup> output synapses in the distal dendritic domain also decreased significantly for deprived neonatal-born GCs (at 28 d.p.i., Fig. 6). These findings are similar to the effects caused by sensory deprivation in immature adult-born GCs. However, whereas early olfactory deprivation increased PSDG<sup>+</sup> proximal synapses in adult-born GCs, it did not trigger any changes in the proximal domain of neonatal-born neurons (Fig. 5A).

After synaptic development, 3 weeks of sensory deprivation only evokes changes in densities of glutamatergic synapses in the proximal, but not in the basal and distal domain of adult-born GCs (Kelsch et al., 2009). As neonatal-born GCs displayed an increase in heterogeneity that occurred slowly over several months (Fig. 1), we first examined whether a longer period of “late deprivation” might evoke changes in the basal and distal domain of adult-born GCs. We observed that “late deprivation” of adult-born GCs for 7–9 weeks did not cause any change in the synaptic densities in the distal (mean  $\pm$  SD:

deprived:  $0.322 \pm 0.074$  and control (nondeprived) bulb:  $0.316 \pm 0.125$  PSDG<sup>+</sup> clusters/ $\mu\text{m}$ ,  $P = 0.87$ , both  $n = 14$  from 5 animals) and basal domains (mean  $\pm$  SD: deprived:  $0.349 \pm 0.146$  and control bulb:  $0.320 \pm 0.092$  PSDG<sup>+</sup> clusters/ $\mu\text{m}$ ,  $P = 0.52$ , both  $n = 14$  from 5 animals). In addition, synaptic densities of adult-born GCs remained increased in the proximal domain after 9 weeks of sensory deprivation (mean  $\pm$  SD: deprived:  $0.746 \pm 0.230$  and control bulb:  $0.561 \pm 0.138$  PSDG<sup>+</sup> clusters/ $\mu\text{m}$ ,  $P = 0.01$ , both  $n = 14$  from 5 animals).

In contrast to adult-born GCs, the synaptic densities of neonatal-born GCs become progressively more heterogeneous over extended periods of time. This suggests that neonatal-born GCs may be able to reorganize their synaptic inputs for longer periods of time than adult-born GCs. Thus, we investigated whether neonatal-born GCs, like adult-born GCs, had a restricted period during which extensive changes in their synaptic organization occurred, or whether mature neonatal-born GCs retained the ability to change their synaptic organization in response to sensory deprivation.

We labeled GCs in the SVZ of newborn animals (P5) and started unilateral naris occlusion only when animals reached adulthood. “Late deprivation” of neonatal-born GCs started at P75 resulted in a significant loss of basal and distal synapses after 7 weeks of sensory deprivation (Fig. 5B). In addition, a transient decrease in the density proximal synapses was observed after 3 weeks of deprivation, but this density returned to control levels after 7 weeks of deprivation (Fig. 5B). Thus, late sensory deprivation affected synaptic densities in all dendritic domains of neonatal-born GCs.

These results indicate that mature neonatal-born GCs retain a higher degree of malleability in terms of reorganizing their synaptic densities in response to changes in sensory activity than mature adult-born GCs (Fig. 7), which is consistent with increasing heterogeneity of synaptic densities of mature neonatal-, but not adult-born GCs.

## DISCUSSION

It is generally believed that adult neurogenesis provides a continuous influx of immature neurons that become less plastic as they mature, such that the circuit requires subsequent waves of immature neurons to provide plasticity to store novel information. According to this hypothesis, adult neurogenesis represents the continuous addition of immature neurons with the same properties, regardless of whether they are generated in the developing or adult brain. We observed that, whereas adult-born GCs maintained stable synaptic densities soon after integrating into the circuit, in line with this

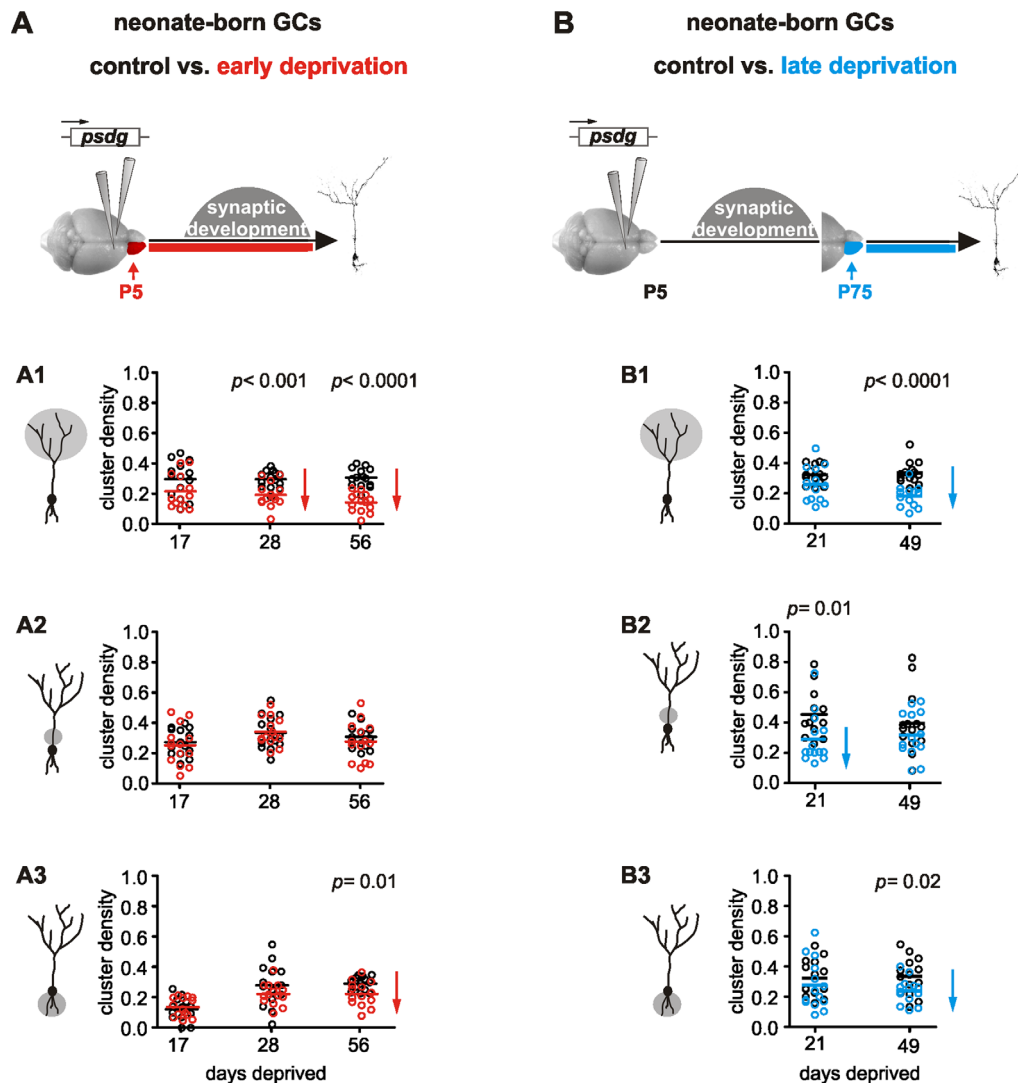


**Figure 5.** The glutamatergic input synapse densities of neonatal-born GCs is affected by sensory deprivation occurring both during and after their integration in the circuit. **A:** Early sensory deprivation: Progenitor cells were infected with retroviruses in the subventricular zone at P5 in combination with unilateral naris occlusion on the same day. Genetically labeled GCs were examined at different days of occlusion. Scatterplot and mean density of PSDG<sup>+</sup> clusters (clusters/ $\mu\text{m}$ ) of neonatal-born GCs in sensory-deprived and contralateral control olfactory bulbs (red and black circles, respectively). Statistical significance is only indicated if  $P < 0.05$  ( $t$ -test) and highlighted by arrows. The three main dendritic domains were analyzed separately (from top): distal (A1), proximal (A2), or basal (A3) domain. **B:** Late sensory deprivation: Progenitor cells were infected with retroviruses in the subventricular zone at P5 and unilateral naris occlusion started at P75. Genetically labeled GCs were examined at different survival days after occlusion. Scatterplot and mean density of PSDG<sup>+</sup> clusters (clusters/ $\mu\text{m}$ ) of neonatal-born GCs in sensory-deprived and contralateral control olfactory bulbs (blue and black circles, respectively). Statistical significance is only indicated if  $P < 0.05$  ( $t$ -test). The three main dendritic domains were analyzed separately (from top): distal (B1), proximal (B2), or basal (B3) domain.

hypothesis, the density of synaptic inputs in neonatal-born GCs keeps changing for many subsequent months. In addition, mature neonatal-, but not adult-born GCs, remained malleable to reorganize their synaptic densities in all dendritic domains in response to manipulation of sensory input. Thus, suggesting neonatal- and adult-born GCs not only differ in their initial pattern of synaptic development, but also thereafter when they function as mature neurons in the OB. In this study we compared

neurons of the same ages (1, 2, and 12 months after being born in the SVZ) that were generated in either adult and neonatal animals. Future studies may further explore the dynamics of long-term changes in the same neurons over time to also examine subtle differences in addition to changes in cell-to-cell variability. Study of long-term in vivo imaging of genetically labeled synapses, however, is currently limited to more superficial periglomerular neurons (Livneh et al., 2009).

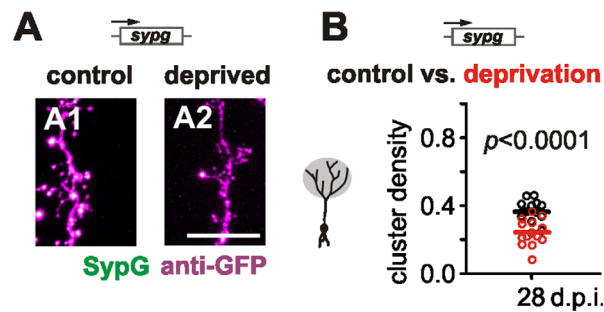


**Figure 6.** The output synapse densities of neonatal-born GCs is affected by sensory deprivation. **A:** Early sensory deprivation: Progenitor cells were infected with retroviruses in the SVZ at P5 in combination with unilateral naris occlusion on the same day. Genetically labeled nondeprived (A1) and deprived (A2) GCs were examined at 28 d.p.i. **B:** Scatterplot and mean density of SypG<sup>+</sup> clusters (clusters/ $\mu\text{m}$ ) of neonatal-born GCs in sensory-deprived and contralateral control olfactory bulbs (red and black circles, respectively, *t*-test). Scale bar = 10  $\mu\text{m}$ .

In this study we used confocal microscopy to image and quantify the densities of the genetically labeled cluster of PSD-95:GFP. In particular, we observed pronounced changes in the density of synapses on neonatal-born GCs over a period of 1 year of survival. Several mechanisms may account for these changes in synaptic density. First, the changes in synaptic density may be due to a net increase or decrease in the number of synapses. Second, these changes in density may be due to a reorganization of the synaptic clusters (splitting or merging of clusters) over time (Woolf and Greer, 1991), without a net change in the total number of postsynaptic receptors. Third, the changes in synaptic density may be due to a progressive accumulation of PSD-95 in mature synapses as neurons still may change their synaptic strength for long periods of time after their integration into brain circuits (Kim et al., 2007). According to this scenario, more synaptic clusters may become detectable by microscopy as more PSDG molecules are trapped in a synapse. However, regardless of the mechanism responsible for the change in synaptic density in neonatal-born GCs, such changes were not observed in adult-born GCs over the same period of time, indicating that they do not display the same malleability as neonatal-born GCs. Future experiments using complementary approaches will help to further understand the significance of the progressive increase in cell-to-cell variability in mature neonatal-born GCs.

### Sources of synaptic heterogeneity

Synaptic densities in the dendritic domains of neonatal-born GCs become increasingly heterogeneous throughout the life of the animal long after these neurons mature. Heterogeneity in the synaptic organization of

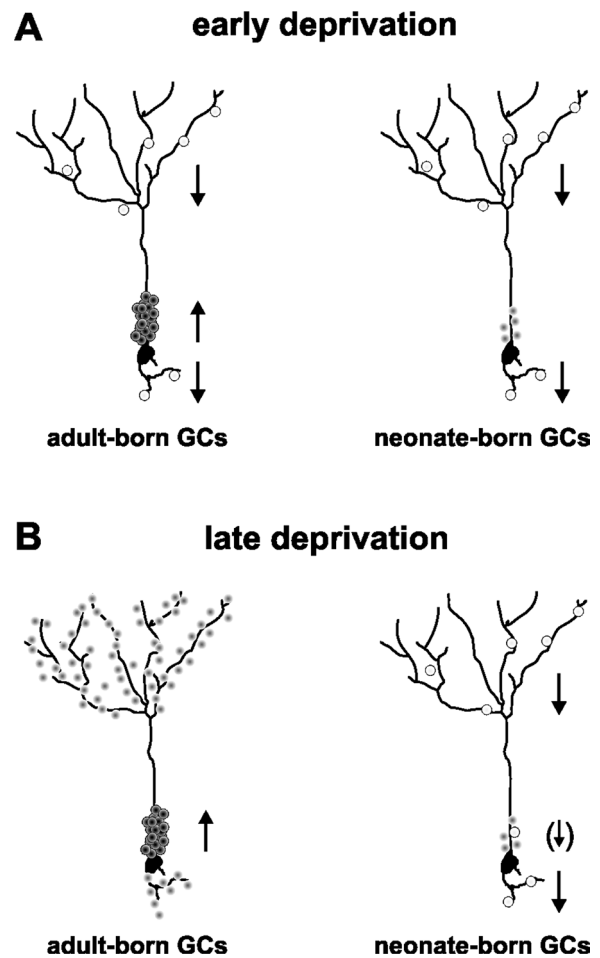


**Figure 7.** Sensory deprivation differently changes the synaptic densities in neonatal- and adult-born GCs. **A:** Early sensory deprivation reduced synaptic densities in the distal and basal domain of both neonatal- and adult-born GCs. However, early sensory deprivation increased the synaptic density in the proximal domain of adult-born GCs but had no effect in neonatal-born GCs. **B:** In adult-born GCs, when sensory deprivation started after the completion of synaptic development, the only detectable changes were increases in the density of glutamatergic input synapses in the proximal domain. In contrast, in neonatal-born GCs, sensory deprivation that started only after their integration into the circuit decreased the density of glutamatergic synapses in their basal and distal domains and transiently in their proximal domain.

neonatal-born GCs can be attributed to several factors that shape the formation, stabilization, or loss of synapses. These factors include cell-intrinsic factors such as a high intrinsic level of cell-to-cell variability (Raser and O'Shea, 2005), as well as extrinsic factors such as variability in the number of presynaptic axons in the immediate proximity of individual synapses (Stepanyants and Chklovskii, 2005). Neonatal-born GCs retain the ability to change their synaptic densities in their basal and proximal dendritic domains over long periods of time in response to changes in activity (Fig. 2C). Perhaps as a

result of this long-lasting synaptic plasticity, their synaptic densities display increasing variability between individual neurons over time. In contrast, adult-born GCs acquire their final density of synapses within 1 month after their birth, and display no change in cell-to-cell variability in the density of their synapses once they mature (Fig. 2C). Thus, once they mature, adult-born GCs appear to acquire one “flavor” that under normal circumstances does not change over prolonged periods of time. This suggests that these neurons may become hardwired soon after their differentiation to perform a defined computational task over the neuron’s lifetime. In contrast, mature neonatal-born GCs seem to change their “flavors” over time, suggesting a more dynamic wiring that may reflect changes in their computational demands during their lifespan.

### Neonatal- and adult-born GCs may perform different functions in the OB

Different forms of plasticity of mature adult-born GCs in comparison with neonatal-born GCs are underscored by widespread changes in the synaptic organization of neonatal-born GCs in contrast to the restricted remodeling of adult-born GCs caused by late sensory deprivation. When late sensory deprivation, which is induced postdifferentiation, was performed, widespread changes in synaptic wiring of neonatal-born GCs were observed only after a long period of deprivation, in contrast to the rapid changes seen during early sensory deprivation. This is reminiscent of the slow increase in heterogeneity of synaptic densities in these neurons under nondeprived conditions. Interestingly, although we observed a decrease in synaptic density in the distal domain of neonatal-born GCs triggered by late sensory deprivation, in nondeprived animals there was little change in the variability or mean density of these distal synapses over time. It is possible that the distal synapses of neonatal-born GCs only change their density if the activity of the OB circuit is perturbed in an extreme manner, such as by sensory deprivation. Alternatively, it is possible that the changes that occur in dendrodendritic synapses under nondeprived conditions, in contrast to the changes seen in axodendritic synapses, are too subtle to be detected using our methods.

Axonal projections from higher olfactory areas to GCs (“axodendritic inputs”) are thought to provide context-related information like reward or aversion that shapes early odor processing in the OB (Kiselycznyk et al., 2006; Su et al., 2009). Activation of axodendritic inputs depolarizes and globally excites GCs. Global excitation of GCs facilitates inhibition of tufted and mitral cells (Chen et al., 2000; Halabisky and Strowbridge, 2003) and thereby axo-

dendritic inputs may shape odor processing (Laurent, 1999). The increasing heterogeneity in the axodendritic synaptic densities of neonatal-born GCs and their ability to sustain deprivation-induced plasticity suggest that they can adapt their synaptic wiring to changing demands over the animals’ lifespan. In particular, reorganizing their axodendritic inputs may change the context-related information that activates neonatal-born GCs during odor processing at different stages of the animal’s life.

In contrast to neonatal-born GC, adult-born GCs may use activity-dependent mechanisms within a restricted window of time to allow sensory information to shape synaptic wiring during their differentiation. After their integration into the circuit, it appears that adult-born GCs’ stereotypical synaptic organization remains mostly unperturbed for the rest of their existence. Such a “snapshot” model of synaptic wiring would fit with recent observations that adult-born GCs may be involved in forming long-lasting memories acquired at one point in the life of the animal (Mak and Weiss, 2010). Interestingly, whereas few neonatal-born GCs die after they mature throughout life of the animal, adult-born GCs show a continuous turnover throughout life, potentially explaining the low numbers of 1-year-old adult-born GCs that we found (Fig. 2A). Such differences in turnover would match that “snapshots” taking adult-born GCs are discarded after some time (Petreanu et al., 2002; Lemasson et al., 2005; Mouret et al., 2009), whereas neonatal-born GCs adapt their wiring over time and stay in the circuit. In summary, the different degrees of plasticity between neonatal- and adult-born GCs suggest a role of neonatal-born GCs as life-long learners and of adult-born GCs as “capture-and-replay” modules in the OB circuit.

### LITERATURE CITED

- Altman J. 1962. Are new neurons formed in the brains of adult mammals? *Science (New York)* 135:1127–1128.
- Brandstatter JH, Fletcher EL, Garner CC, Gundelfinger ED, Wassle H. 1999. Differential expression of the presynaptic cytomatrix protein Bassoon among ribbon synapses in the mammalian retina. *Eur J Neurosci* 11:3683–3693.
- Chen WR, Xiong W, Shepherd GM. 2000. Analysis of relations between NMDA receptors and GABA release at olfactory bulb reciprocal synapses. *Neuron* 25:625–633.
- Gray NW, Weimer RM, Bureau I, Svoboda K. 2006. Rapid redistribution of synaptic PSD-95 in the neocortex in vivo. *PLoS Biol* 4:e370.
- Halabisky B, Strowbridge BW. 2003. Gamma-frequency excitatory input to granule cells facilitates dendrodendritic inhibition in the rat olfactory bulb. *J Neurophysiol* 90:644–654.
- Hinds JW. 1970. Reciprocal and serial dendrodendritic synapses in the glomerular layer of the rat olfactory bulb. *Brain Res* 17:530–534.
- Kelsch W, Lin CW, Lois C. 2008. Sequential development of synapses in dendritic domains during adult neurogenesis. *Proc Natl Acad Sci U S A* 105:16803–16808.

- Kelsch W, Lin CW, Mosley CP, Lois C. 2009. A critical period for activity-dependent synaptic development during olfactory bulb adult neurogenesis. *J Neurosci* 29:11852–11858.
- Kim MJ, Futai K, Jo J, Hayashi Y, Cho K, Sheng M. 2007. Synaptic accumulation of PSD-95 and synaptic function regulated by phosphorylation of serine-295 of PSD-95. *Neuron* 56:488–502.
- Kiselycznyk CL, Zhang S, Linster C. 2006. Role of centrifugal projections to the olfactory bulb in olfactory processing. *Learn Mem (Cold Spring Harbor, NY)* 13:575–579.
- Laurent G. 1999. A systems perspective on early olfactory coding. *Science (New York)* 286:723–728.
- Lemasson M, Saghatelian A, Olivo-Marin JC, Lledo PM. 2005. Neonatal and adult neurogenesis provide two distinct populations of newborn neurons to the mouse olfactory bulb. *J Neurosci* 25:6816–6825.
- Livneh Y, Feinstein N, Klein M, Mizrahi A. 2009. Sensory input enhances synaptogenesis of adult-born neurons. *J Neurosci* 29:86–97.
- Lois C, Alvarez-Buylla A. 1993. Proliferating subventricular zone cells in the adult mammalian forebrain can differentiate into neurons and glia. *Proc Natl Acad Sci U S A* 90:2074–2077.
- Luskin MB. 1993. Restricted proliferation and migration of postnatally generated neurons derived from the forebrain subventricular zone. *Neuron* 11:173–189.
- Mak GK, Weiss S. 2010. Paternal recognition of adult offspring mediated by newly generated CNS neurons. *Nat Neurosci* 13:753–758.
- Meyer MP, Smith SJ. 2006. Evidence from in vivo imaging that synaptogenesis guides the growth and branching of axonal arbors by two distinct mechanisms. *J Neurosci* 26:3604–3614.
- Mouret A, Lepousez G, Gras J, Gabellec MM, Lledo PM. 2009. Turnover of newborn olfactory bulb neurons optimizes olfaction. *J Neurosci* 29:12302–12314.
- Mori K. 1987. Membrane and synaptic properties of identified neurons in the olfactory bulb. *Prog Neurobiol* 29:275–320.
- Niell CM, Meyer MP, Smith SJ. 2004. In vivo imaging of synapse formation on a growing dendritic arbor. *Nat Neurosci* 7:254–260.
- Nissant A, Bardy C, Katagiri H, Murray K, Lledo PM. 2009. Adult neurogenesis promotes synaptic plasticity in the olfactory bulb. *Nat Neurosci* 12:728–730.
- Northcutt KV, Wang Z, Lonstein JS. 2007. Sex and species differences in tyrosine hydroxylase-synthesizing cells of the rodent olfactory extended amygdala. *J Comp Neurol* 500:103–115.
- Petreanu L, Alvarez-Buylla A. 2002. Maturation and death of adult-born olfactory bulb granule neurons: role of olfaction. *J Neurosci* 22:6106–6113.
- Raser JM, O'Shea EK. 2005. Noise in gene expression: origins, consequences, and control. *Science (New York)* 309:2010–2013.
- Regus-Leidig H, Tom Dieck S, Specht D, Meyer L, Brandstatter JH. 2009. Early steps in the assembly of photoreceptor ribbon synapses in the mouse retina: the involvement of precursor spheres. *J Comp Neurol* 512:814–824.
- Sanes JR. 1989. Analysing cell lineage with a recombinant retrovirus. *Trends Neurosci* 12:21–28.
- Serrats J, Sawchenko PE. 2006. CNS activational responses to staphylococcal enterotoxin B: T-lymphocyte-dependent immune challenge effects on stress-related circuitry. *J Comp Neurol* 495:236–254.
- Sheng M. 2001. Molecular organization of the postsynaptic specialization. *Proc Natl Acad Sci U S A* 98:7058–7061.
- Smeets WJ, Gonzalez A. 2000. Catecholamine systems in the brain of vertebrates: new perspectives through a comparative approach. *Brain Res Brain Res Rev* 33:308–379.
- Stepanyants A, Chklovskii DB. 2005. Neurogeometry and potential synaptic connectivity. *Trends Neurosci* 28:387–394.
- Sturgill JF, Steiner P, Czervionke BL, Sabatini BL. 2009. Distinct domains within PSD-95 mediate synaptic incorporation, stabilization, and activity-dependent trafficking. *J Neurosci* 29:12845–12854.
- Su CY, Menuz K, Carlson JR. 2009. Olfactory perception: receptors, cells, and circuits. *Cell* 139:45–59.
- Sudhof TC, Jahn R. 1991. Proteins of synaptic vesicles involved in exocytosis and membrane recycling. *Neuron* 6:665–677.
- Woolf TB, Shepherd GM, Greer CA. 1991. Serial reconstructions of granule cell spines in the mammalian olfactory bulb. *Synapse* 7:181–192.